Initial Performance of the PHENIX Hadron Blind Detector at RHIC

C.Woody, B.Azmoun, C-Y.Chi, Z.Citron, M.Connors, M.Durham, T.Hemmick, A.Iordanova, J.Kamin, B.Lewis, A.Milov, M.Naglis, V.Pantuev, R.Pisani, M.Proissl, I.Ravinovich, S.Rolnick, T.Sakaguchi, D.Sharma, S.Stoll, J. Sun, I.Tserruya

Abstract— **The PHENIX Hadron Blind Detector (HBD) was successfully operated during the 2009 high energy polarized proton run at RHIC. This was the first data taking run after the detector was rebuilt following its first commissioning run in 2007. The detector was operated for several months under actual beam conditions and showed greatly improved performance over the commissioning run. Results are given on the operation of the detector, determination and calibration of the gain using scintillation light produced by charged particles in CF_4, stability of the CsI photocathodes, the ability to identify single and double electrons using the signal from Cherenkov light, and the level of sensitivity of the detector to charged hadrons. A description is also given on the methods used to reconstruct the detector that led to its improved performance.**

I. INTRODUCTION

THE PHENIX Hadron Blind Detector (HBD) is a high performance Cherenkov detector that will be used to identify electrons resulting from Dalitz pairs and conversions in heavy ion and proton-proton collisions at RHIC [1]. It will allow an overall improvement of at least a factor of 20 in the signal to background ratio for the measurement of electron-positron pairs in the low mass pair continuum and from the decay of light vector mesons (ρ, ω and ϕ). The HBD uses photosensitive GEM detectors to detect Cherenkov light from relativistic electrons while producing minimal signals for charged hadrons, making it essentially "hadron blind". It is a windowless, proximity focused Cherenkov counter that uses pure CF_4 as both the radiator gas and as the operating gas for the GEM detectors, which results in an extremely large bandwidth of UV sensitivity (from ~ 6.0 to 11.5 eV) and a high photoelectron yield for identifying electrons.

Manuscript submitted on November 13, 2009. This work was supported in part by the U.S. Department of Energy under Prime Contract No. DE-AC02-98CH10886.

A.Milov, M.Naglis, I.Ravinovich, D.Sharma and I. Tserruya are with the Department of Particle Physics, Weizmann Institute of Science, Rehovot, Israel

B.Azmoun, R.P.Pisani, T.Sakaguchi, A.Sickles, S.Stoll and C.Woody are with Brookhaven National Laboratory, Upton, NY.

Z.Citron, M.Connors, M.Durham, T.Hemmick, B.Lewis, J.Kamin, V. Pantuev, M.Proissl and J. Sun are with the Physics Department, Stony Brook University, Stony Brook, New York.

A.Iordanova and S.Rolnick are with the University of California Riverside, Riverside, CA.

C.-Y. Chi is with Nevis Labs, Columbia University, Irvington, NY.

The overall design of the detector has been described previously [2-4]. It was initially installed into PHENIX and operated for its first commissioning during Run 7 at RHIC in early 2007. However, during that run, a number of problems were discovered related to the high voltage system and the way the detector was operated that resulted in severe damage to many of the GEMs. As a result, the entire detector was removed from PHENIX and rebuilt after a long and careful study to determine the cause of the problems. The rebuilt detector was then reinstalled into PHENIX and operated successfully during the Run 9 polarized proton run at RHIC in the winter and spring of 2009. The detector showed greatly improved performance as well as high voltage stability compared to the 2007 run, and we feel that the initial problems with the detector have now been solved.

In this paper, we will describe the problems encountered in Run 7 and how the solutions were implemented for Run 9. We will also give some initial performance results measured in Run 9 that indicate the detector will meet our requirements for measuring electron pairs in heavy ion collisions. As a result, we feel that the detector is now ready to be used for the first dedicated low mass dilepton pair measurement in heavy ion collisions at RHIC, which will be carried out during Run 10 beginning in late 2009.

II. HBD OPERATION

Figure 1 shows the basic structure of the HBD photosensitive GEM detectors. Each detector module consists of a triple GEM stack in which the top surface of the top GEM is coated with a ~ 300 nm thick layer of CsI that acts as a photocathode. A mesh electrode is placed above the top GEM which allows an electric field to be applied that causes the ionization produced in this gap to be transported either into the GEM stack, which we denote *Forward Bias*, making the detector sensitive to charged particles, or away from the GEM stack and collected by the mesh, which we denote as *Reverse Bias,* making the detector essentially blind to charged hadrons (hence the term *Hadron Blind*). However, even in reverse bias mode, there is some sensitivity to hadrons due to the ionization produced in a very thin (~ 100 μm) layer above the top GEM which is collected into the GEM stack, and from ionization produced in the first transfer gap, which receives less than the full gain of the stack, but still contributes a significant signal.

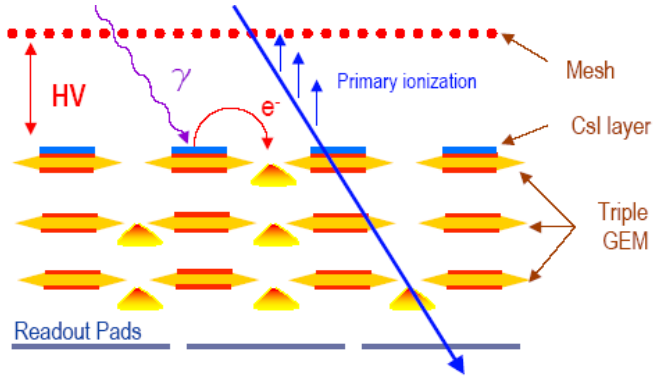

Fig. 1 Configuration of GEM detectors and CsI photocathodes in the HBD. In *Forward Bias* mode, a larger negative voltage is applied to the mesh than the top GEM and ionization in the first gap is collected and amplified by the GEM stack. In *Reverse Bias*, a lower negative voltage is applied to the mesh, and ionization in the gap is collected by the mesh, making the detector essentially *Hadron Blind*.

In PHENIX, the HBD is used to suppress the combinatorial background coming from π^0 Dalitz decays and gamma conversions in order to make a precision measurement of the low mass electron pair spectrum in heavy ion collisions. In order to do so, one needs to suppress this background by a factor of ~ 100 in the mass region from ~ 300 MeV < m_{ee} < 1 GeV. This requires a single electron detection efficiency greater than ~ 90%, and a pair efficiency ≥ 80%.

The PHENIX Central Magnet consists of an inner and outer magnet coil that can create an essentially field free region inside the HBD. In such a configuration, electron pairs from Dalitz decays and conversions do not open up and travel together through the HBD. Since the HBD is a proximity focused device (i.e., there is no mirror), these two tracks produce a cluster of pad hits equivalent to two electrons, which one attempts to differentiate from isolated single electron clusters from the low mass pair signal. The ability to resolve single and double electron clusters, while preserving high electron detection efficiency and good hadron rejection, is therefore critical in the operation of the HBD and its ability to provide the necessary background suppression for an electron pair measurement in heavy ion collisions.

III. PROBLEMS ENCOUNTERED IN RUN 7

The assembly of the HBD detector was carried out inside a large clean tent at Stony Brook University. Initially, the final assembly and installation of the GEMs was done inside a glove box within the clean tent because of the sensitivity of the CsI coated GEMs to air. While great care was taken to clean the glove box before and during assembly, dust invariably accumulates inside as materials and detector components are brought in. The particle count inside the glove box was typically better than Class 100 (< 100 0.5 µm particles/m^3), but was significantly higher in certain areas. In addition, each completed GEM stack was initially tested inside a separate vessel inside the glove box before being installed into the HBD. This test vessel was therefore a place where dust could easily accumulate and contaminate otherwise clean GEMs.

It is well known that GEM detectors are susceptible to spontaneous discharging, but the accumulation of dust can make them even more sensitive to this effect. We feel that this was the basic problem with the GEMs that we experienced in Run 7. Our procedure for assembling the detector was clean, but not clean enough. The accumulation of dust during the final assembly and testing resulted in GEMs that suffered from frequent discharges that eventually led to more serious problems during their operation.

The relatively minor and usually harmless discharges that occur across the GEM foils were compounded in Run 7 because of the voltage divider that was used to bias the GEM stack. Figure 2 shows this divider, which contained no bleeder resistor for the mesh. Therefore, a small discharge on the GEM leading to a trip would result in a large voltage developing across the mesh to GEM gap as the voltage on the GEM dropped to zero. This resulted in large mesh to GEM sparks, that were exacerbated by the large stored energy of the filter capacitors in both the divider and the high voltage power supply, which ultimately damaged the GEMs. In addition, these large sparks could induce sparks in neighboring modules due to photon propagation in CF_4, causing damage to other modules.

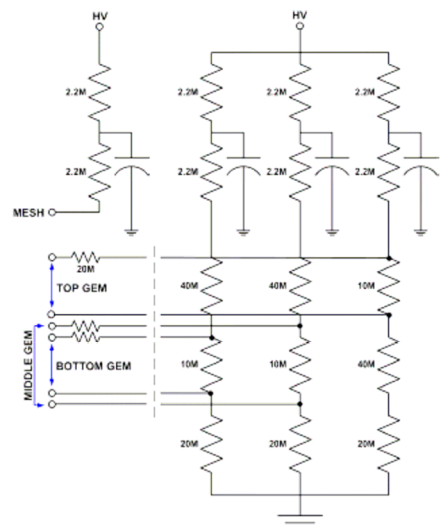

Fig 2. Voltage divider used for biasing the three GEMs and mesh of the HBD modules during Run 7.

An additional problem was also discovered with the LeCroy 1471N high voltage power supply modules that were used to supply voltage to both the mesh and the GEMs. Due to an inherent error in the FPGA code of these modules, the high voltage can suddenly be briefly reapplied for a few tenths of a second after a trip, which resulted in potentially harmful high voltage spikes on the detector. This problem was avoided in Run 9 by introducing a high voltage relay box between the LeCroy 1471N modules and the detector, as described later.

IV. IMPROVEMENTS FOR RUN 9

After its initial commissioning in Run 7, the entire HBD was removed from PHENIX and rebuilt at Stony Brook where a number of substantial improvements were made. First, the glove box was thoroughly cleaned and a more rigorous procedure was implemented for bringing materials and detector components inside the glove box. For the first half of the detector (the East detector), all GEMs were still installed inside the glove box as they had been for Run 7. However, a different procedure was implemented for the second half of the detector (the West detector). This detector was built using a so-called Rapid Method, in which most of the assembly was done near a laminar flow table inside the clean tent (which was the cleanest area inside the tent), and only the CsI coated GEMs were installed inside the glove box. This resulted in much less exposure of all the GEMs to the glove box environment. In Run 9, the West detector generally performed better than the East, and after the end of Run 9, the East detector was rebuilt again using the Rapid Method in preparation for Run 10.

All GEMs were pressure washed with deionized water and pumped on for at least several days before installation. Only the individual GEM foils were tested inside the glove box, rather than testing each completed triple stack as had been done before, which eliminated the use of the separate test vessel where additional exposure to dust could occur. The individual GEM tests consisted of bringing up each GEM to 500 volts in dry nitrogen, which proved to be an entirely adequate test to insure that they would operate well as a complete stack in CF_4.

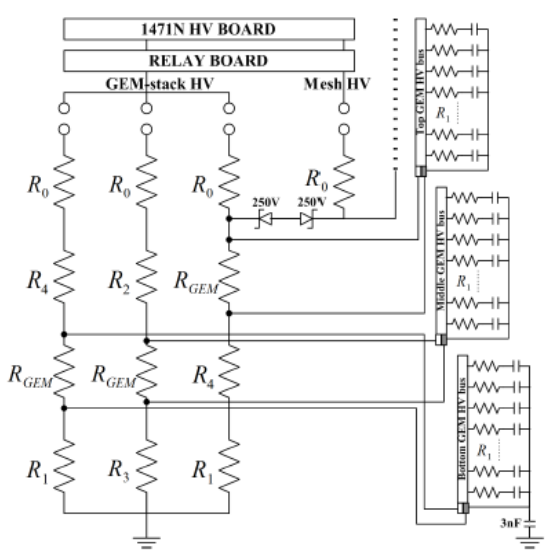

Fig 3. New high voltage system for the HBD in Run 9. The Relay Board used a signal generated by a special trip circuit added to the 1471N to discharge both the mesh and GEM circuits of a given detector module when either tripped.

A new high voltage system was implemented for the HBD in Run 9 that incorporated several new and improved features. This system is shown in Fig 3. Two zener diodes were installed across the mesh to GEM gap that limited the voltage in this gap to < 500V. In addition, a special sensor circuit was added to the LeCroy 1471N modules that was used to provide additional trip protection for both the mesh and the GEMs. The signal from this circuit was sent to a set of high voltage relays that would discharge both the mesh and GEMs of a given detector module whenever either the mesh or the GEM would trip. The values of the resistors of the voltage divider were also changed to increase the voltages in the transfer gaps and induction gap, which provided additional effective gain, while allowing the GEMs themselves to operate at somewhat lower voltage.

In addition to these hardware changes, a new high voltage control program was written that provided excellent control of the high voltage to each module [5], allowing the voltage across each GEM and the mesh to be set with a precision ~ 1 volt.

V. OPERATION IN RUN 9

In order to optimize the performance of the HBD, a number of operational parameters needed to be determined. These included setting the operating voltage for each module, stabilizing the gas gain due to pressure and temperature variations, optimizing the photoelectron collection and hadron rejection of each module, and monitoring the gas quality and quantum efficiency of the photocathodes.

The gas gain of each module was determined using the scintillation light produced in CF_4 by charged particles from the primary collisions. In low multiplicity proton-proton collisions, this scintillation light produces single pad hits on the readout plane corresponding to single photoelectrons. These photoelectrons produce an essentially exponential pulse height distribution, which can be fit, and the inverse slope parameter of this fit gives a measure of the gas gain. Figure 4 gives an example of this distribution for a typical module.

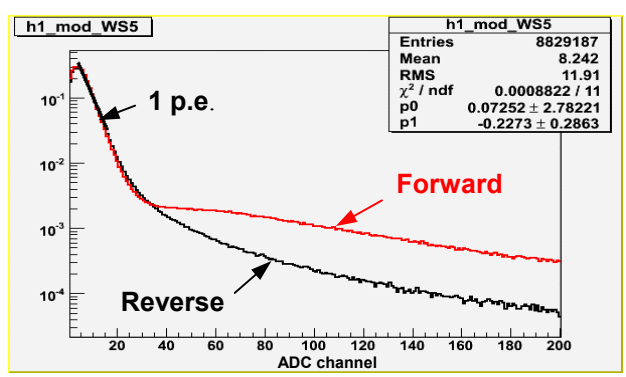

Fig 4. Pulse height distribution for a typical module showing scintillation component (exponential) and ionization tail for forward and reverse bias.

The gas gain was determined by fitting the single photoelectron part of this distribution for each module, and was monitored continuously throughout the run. In addition, with higher statistics from the entire run, the pad by pad gain calibration could also be determined using this method. This calibration was determined once for the run and used to equalize the response of all pads across the detector.

Also shown in figure 4 are the tails of the pulse height distribution for both forward and reverse bias conditions. The ionization signal is clearly much larger in forward bias due to the charge collected in the gap between the top GEM and the mesh. The ionization signal, as well as the photoelectron collection efficiency, is strongly dependent on the voltage across this gap. As discussed in Ref [2], the ionization signal drops very quickly as the gap voltage becomes negative, while the photoelectron collection efficiency drops much more slowly. The operating point which gives the best photoelectron collection efficiency and minimal hadron response is very close to zero volts in this gap, and needs to be set for each module individually in order to optimize its performance.

The mesh to GEM voltage was set for each module by taking a series of special runs where the gain of each module was kept constant and the mesh to GEM gap voltage was varied. Figure 5 shows the data for a typical module. The optimal voltage was set to be the minimal voltage needed to reduce the ionization tail to its minimal value. This required setting this voltage to a precision of ~ 5 V out of ~ 4000 V applied to the voltage divider, or ~ 0.1%.

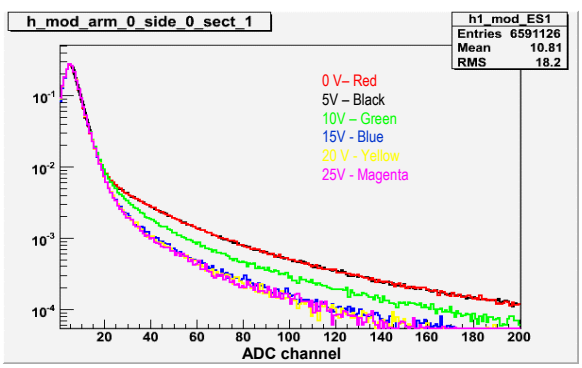

Fig 5. Voltage scan for a typical module (ES1) performed in order to optimize the voltage in the gap between the mesh and top GEM for minimum sensitivity to hadrons and maximum photoelectron efficiency.

One of the most important parameters determining the performance of the detector is the CsI quantum efficiency. Rebuilding the detector required redepositing the CsI photocathodes on all of the top GEMs using the evaporator at Stony Brook [4]. Figure 6 shows the quantum efficiency curve measured for one of the new photocathodes compared to our reference, and indicates that good quantum efficiency was again achieved.

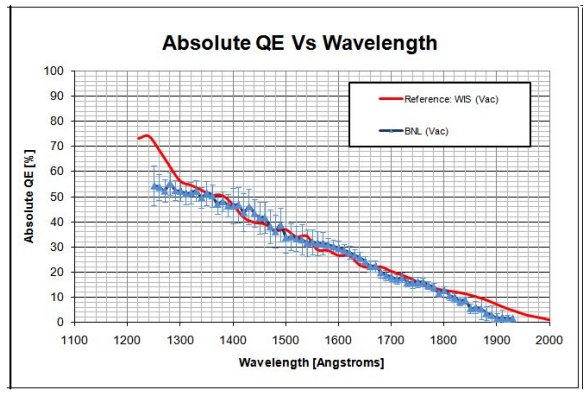

Fig 6. Typical quantum efficiency curve for one of the new photocathodes produced at Stony Brook for the rebuilt detector compared to our reference.

It was also important to maintain the quantum efficiency of the detector throughout the run. This required keeping the water and oxygen levels in the detector as low as possible. However, due to the large amount of kapton in the GEMs and FR4 used in vessel of the HBD, there is considerable outgassing of water from inside the detector itself. The HBD uses a sophisticated recirculating CF_4 gas system to remove water and oxygen from the gas while minimizing expensive CF_4 gas consumption [6]. For Run 9, the flow rate in this system was increased to ~ 4 lpm to each detector, which allowed maintaining the water levels to ~ 30 ppm and the oxygen level to < 5 ppm. This not only helped preserve the quantum efficiency of the photocathodes, but also improved the UV transmission of the gas, which increased the overall photoelectron yield.

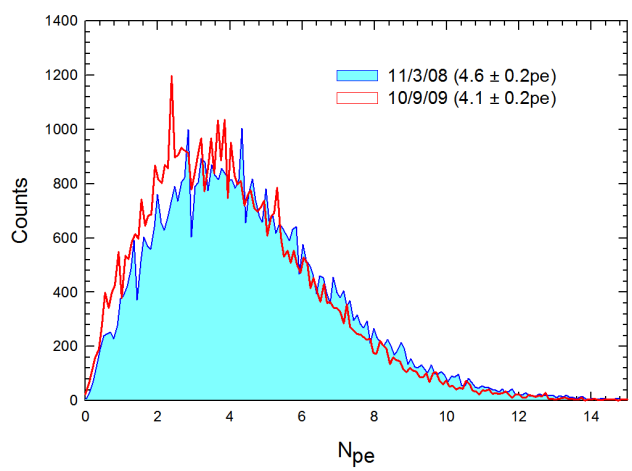

Fig 7. Photoelectron spectrum for the photocathode of the West detector measured with the Scintillation Cube [7] at the beginning of Run 9 (11/3/08) and approximately 11 months later (10/9/09). The photoelectron yield is a measure of the quantum efficiency of the photocathode, which remained essentially unchanged over this period.

In order to monitor the quantum efficiency of the photocathodes in situ, a device known as the "Scintillation Cube" was installed in each half of the detector [7]. This device illuminated a limited region of the photocathode of one of the modules with scintillation light from CF_4 and allowed a determination of the relative quantum efficiency. It was used to measure the quantum efficiency before, during and after the run. Figure 7 shows the photoelectron yield, which is proportional to the quantum efficiency, for the West detector measured at the beginning of Run 9 and approximately 11 months later. The yield dropped from 4.6 ± 0.2 pe to 4.1 ± 0.2 pe, indicating a decrease of ~ 11%. This decrease is essentially within the errors of the measurement, and does not represent a serious degradation in terms of the overall performance of the detector.

VI. PERFORMANCE IN RUN 9

The HBD was operated during Run 9 from February to July of 2009. During that time, PHENIX collected approximately 1.5 billion minimum bias events as well as 3 billion electron trigger events. These events were used to study the detector performance, and will also be used to measure the low mass electron pair spectrum in proton-proton collisions that will be used as a comparison for the measurement in Au-Au collisions in Run 10.

One basic requirement in the analysis of the data is the need to match tracks in the PHENIX Central Arm Spectrometer to cluster hits in the HBD. This was studied using tracks found in the Central Arm and projecting them onto the readout plane of the HBD. Figure 8 shows the results. The matching resolution in ϕ and z is ~ 1 cm, which is consistent with the resolution one would expect from the pad size (hexagonal pad dimension of a = 1.55 cm, implying $\sigma \sim 2a/\sqrt{12} = 0.9$ cm).

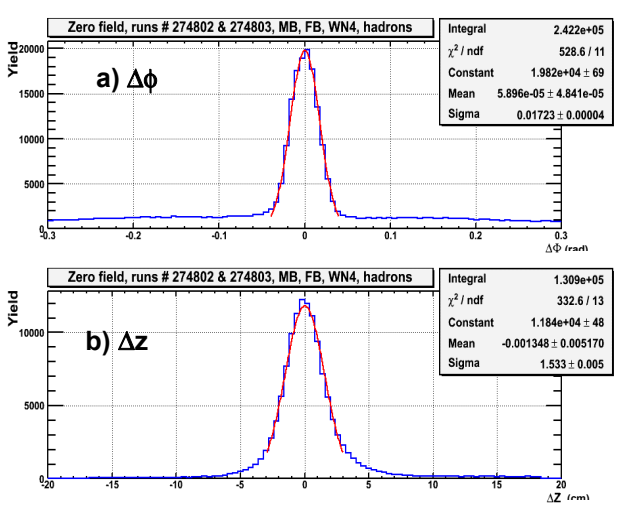

Fig. 8 Matching resolution for tracks found in the PHENIX Central Arm Spectrometer with clusters in the HBD: a) ϕ (azimuthal direction) b) z (longitudinal direction).

The primary performance requirement for the HBD is the ability to separate single and double electron clusters. This was studied using a clean sample of Dalitz pairs selected in the mass region m_{ee} < 150 MeV and looking at either single or double electron clusters. Single electron clusters were selected using an isolation cut and requiring a good match to a well identified electron measured in the Central Arms. Double electron clusters were due to pairs which did not open up in the low central field region. Figure 9 shows these two spectra. The single electron spectrum shows a peak at ~ 22 pe, while the double electron spectrum peaks at ~ 40 pe. This gives very good separation between the two, and will provide an excellent ability to identify single and double electrons in the final physics analysis.

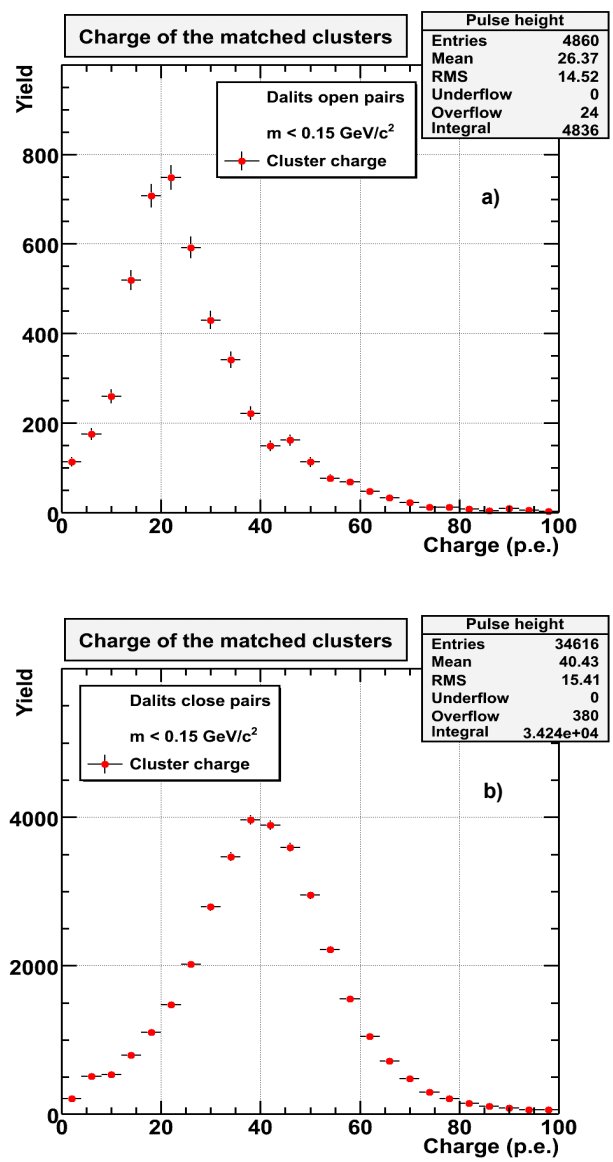

Fig. 9 Photoelectron spectrum for a) single electrons and b) double electrons from Dalitz pairs identified using the PHENIX tracking detectors.

It is also worth noting that the photoelectron yield for single electrons is essentially at the theoretical limit for what we expect given the known efficiencies of the detector. This can be estimated using the known Cherenkov spectrum, applying the wavelength cutoff for CF_4 (108 nm), convoluted with the wavelength dependent quantum efficiency curve (Fig 6), and accounting for the transmission loss in the gas (which is dependent on the ppm levels of water and oxygen), the transmission of the mesh (90%), the transmission of the GEMs (83%), and the wavelength dependent photoelectron collection efficiency (~ 66%) [7]. Convoluting all of these factors together gives ~ 25 pe, which is in very good agreement with the measured mean of ~ 26 pe given in Fig. 9. This also gives us confidence that we have reached the optimal limit of performance of the detector under these operating conditions.

Figure 10 shows the hadron response of the detector in reverse bias mode. The peak is below 1 pe, which is small compared to the 22 pe for single electron tracks. This will therefore provide excellent hadron rejection while preserving good electron efficiency.

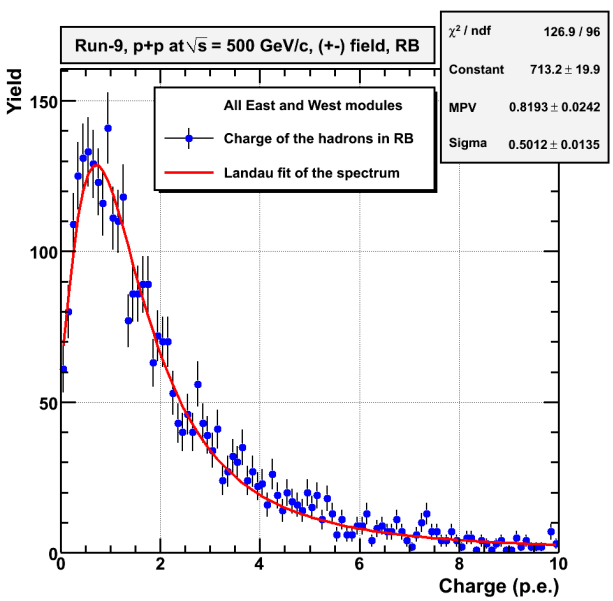

Fig. 10. Hadron response in photoelectrons in reverse bias mode.

By making a cut on the number of photoelectrons in the hadron response, once can compute a hadron rejection factor versus threshold. This is shown in Fig 11. It demonstrates that a rejection factor ~ 50 can be achieved. However, it should be noted that additional cuts, such as the cluster size, can also be applied which will further improve the overall hadron rejection factor.

As mentioned earlier, it is also important to have good electron efficiency for detecting single electrons from low mass pairs and vector mesons, as well as good electron pair efficiency for rejecting Dalitz pairs and conversions. Results on these efficiencies were also determined from the data by

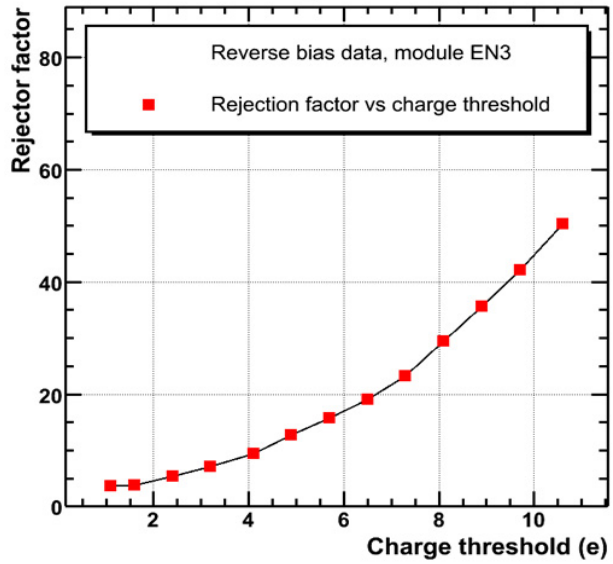

Fig. 11. Hadron rejection factor versus photoelectron threshold.

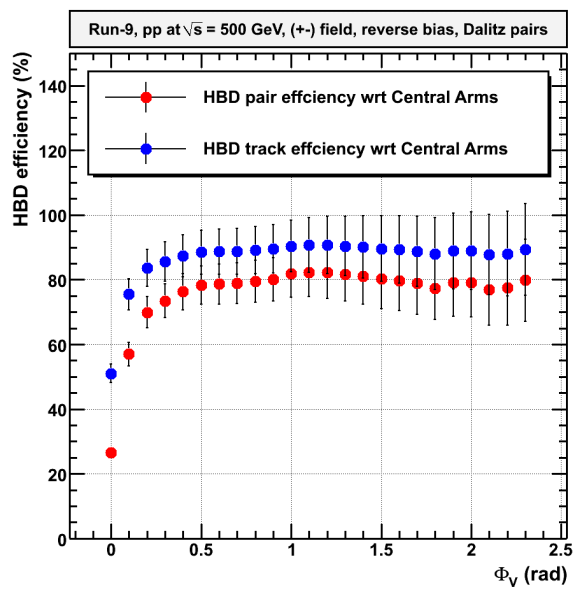

Fig. 12. Efficiency for single electrons and electron pairs from Dalitz decays as a function of the angle between the normal vector to the decay plane and the axial magnetic field.

selecting Dalitz pairs in the very low mass region ($25 < m_{ee} < 50$ MeV) and computing the efficiency for detecting clusters in the HBD compared with tracks found in the Central Arms.

Figure 12 shows the efficiency for singles and pairs as a function of the angle between the normal vector of the decay plane and the axial magnetic field. This angle should be close to zero for conversion pairs. It plateaus at ~ 90% for single electrons and 80% for pairs. These are both at the level required to have good efficiency for detecting the low mass pair and vector meson signal, and for detecting Daliz pairs and conversions in order to reduce the combinatorial background.

VII. SUMMARY

The HBD was rebuilt and refurbished prior to the 2009 polarized proton run at RHIC, and was then reinstalled and operated for more than six months under actual beam conditions. The detector performed very well in virtually all respects, including much improved high voltage stability compared to its previous operation in 2007. We believe this was mainly due to a much higher level of cleanliness and reduction of exposure to dust that was implemented during the reconstruction, as well as to improved operating conditions in terms of high voltage control and gas quality. We achieved a photoelectron yield for single electron tracks that is at the theoretical limited expected given the known efficiencies of the detector. This yield gives good electron efficiency and separation between single and double electrons that are required for Dalitz pair rejection. The response of the detector to hadrons is highly suppressed compared to electrons, as expected for hadron blind operation. The East detector, which was rebuilt for Run 9 using a method that was more prone to dust, did not perform as well as the West detector. However, the East has now been rebuilt again using the same method that was used for the West. Both detectors are now installed in PHENIX, tested and fully operational, and are ready to be used for the first dedicated measurement of low mass electron pairs in heavy ion collisions at RHIC starting in Run 10, which will begin in December of 2009.

VIII. REFERENCES

[1] B.Azmoun et.al., "Conceptual Design Report on a HBD Upgrade for the PHENIX Detector", March 2005, http://www.phenix.bnl.gov/WWW/TPCHBD/HBD_CDR.pdf

[2] A.Kozolov et.al., "Development of a Triple GEM UV Photon Detector Operated in Pure CF_4 for the PHENIX Experiment", Nucl. Inst. Meth. A523 (2004) pp. 345-354.

[3] Z.Frankel et.al., "A Hadron Blind Detector for the PHENIX Experiment at RHIC", Nucl. Inst. Meth. A546 (2005) pp. 466-480.

[4] C.Woody et.al., "Prototype Tests and Construction of the Hadron Blind Detector for the PHENIX Experiment", Conference Record Proceedings of the 2006 IEEE Nuclear Science Symposium, San Diego, CA, October 29 – November 4, 2006 pp. 1557-1561.

[5] M.Prossil, "HBD HV Control and Monitoring System for the PHENIX Experiment at the Relativistic Heavy Ion Collider", Masters of Science Thesis, Stony Brook University, September 2009.

[6] B.Azmoun et.al., "A VUV Gas Transmission Monitor and Recirculating Gas system for the PHENIX Hadron Blind Detector", Conference Record Proceedings of the 2007 IEEE Nuclear Science Symposium, Honolulu, HI, October 27-November 3, 2007, pp 716-719.

[7] B.Azmoun et.al., "Collection of Photoelectrons and Operating Parameters of CsI Photocathode GEM Detectors", IEEE Trans. Nucl. Sci. NS-56, Vol. 3 (2009) pp. 1544-1549.